Published in IET Electric Power Applications
Received on 9th April 2013
Revised on 4th October 2013
Accepted on 11th October 2013
doi: 10.1049/iet-epa.2013.0192

ISSN 1751-8660

Single and double compound manifold sliding mode observers for flux and speed estimation of the induction motor drive

Mihai Comanescu

Division of Business and Engineering, Penn State Altoona, 3000 Ivyside Park, Altoona, PA 16601, USA
E-mail: muc23@psu.edu

Abstract: The study discusses the problem of speed and flux estimation for the induction motor (IM) drive and presents the design of two sliding mode observers (SMO) with compound manifolds. Both observers are developed using the IM model in the stationary reference frame. The first observer is a single-manifold SMO – it estimates the motor fluxes and yields an approximate value of the speed; however, it is not a converging observer. The single-manifold design is transformed into a double-manifold observer by adding extra feedback terms – this leads to a fully convergent observer that also yields an accurate estimate of the speed. The observers are designed using compound manifolds, which are chosen as a combination of the estimated fluxes and current mismatches. Observers with compound manifolds have been rarely investigated because they cannot be designed using a standard procedure; however, they are shown to have interesting properties. Observer uniqueness is also discussed. The methods proposed are suited to a sensorless IM drive control algorithm where the speed, the flux magnitude and the rotor flux angle are needed. The theoretical developments are supported with simulations and experiments.

Nomenclature

ω_r, ω_s	rotor electrical speed and synchronous speed
n_p	number of pole pairs
R_s, R_r	stator, rotor resistances
L_m, L_s, L_r	magnetising, stator and rotor inductances
η	inverse of rotor time constant
λ_r	rotor flux magnitude
α, β	stationary reference frame quantities
d, q	rotational reference frame quantities
^, *	estimated and reference quantity

1 Introduction

The induction motor (IM) is used in various industrial and manufacturing processes, especially to drive pumps, compressors and fans. It is also used in high-performance applications like windmills and hybrid electric vehicles. The squirrel cage motor is very robust, requires almost no maintenance and has a wide torque–speed characteristic.

In applications where accurate speed or torque control is required, the IM is usually fed by a three-phase inverter and is controlled using field-oriented methods (vector control). Field-oriented control allows accurate control of the motor torque and speed and is preferred over scalar (V/Hz) control.

The most popular method for IM vector control is based on rotor field orientation. With this, the rotor flux vector establishes the direction of the d-axis of the synchronous reference frame. The main advantage of rotor field orientation is that the synchronous currents i_d, i_q are decoupled at steady-state (but not during transient); as a result, they can be easily controlled to their reference values.

For that, it is typical to use current control schemes based on proportional-integral controllers, with or without dynamic decoupling [1–6].

To implement the rotor field-oriented control scheme, the angle of the rotor flux is required. This can be obtained by direct field orientation (DFO) or by indirect field orientation (IFO).

The IFO method is based on integrating the motor's slip equation in the synchronous reference frame – for that, it is required to measure the speed and to calculate the slip speed. It is well-known that the angle obtained by IFO is sensitive to the value of the rotor resistance used.

The DFO method obtains the flux angle using the $\tan^{-1}$ function and the projections of the rotor flux on the stationary reference frame. It is typical to estimate the α, β fluxes of the IM model using an observer.

Many such observer designs are available [1–26]. Depending on the approach, these are obtained using linear, non-linear or sliding mode (SM) design methods and perform state or state and speed estimation. Some methods combine estimation with adaptation [3, 6, 8], whereas others also involve parameter estimation [20, 24]. A separate class is that of SM observers (SMOs) [10–15, 17–21, 24–27]; in this case, the estimation is done using discontinuous feedback terms. The SM motion may be enforced on single or multi-dimensional manifolds – SM methods allow for order reduction and provide robustness to uncertainties.

Working with a general n-dimensional system of the type

$$\begin{cases} \dot{x} = \boldsymbol{A}\boldsymbol{x} + \boldsymbol{B}u \\ y = \boldsymbol{C}\boldsymbol{x} \end{cases} \quad (1)$$

It is easy to design a SMO if matrices $\boldsymbol{A}$, $\boldsymbol{B}$, $\boldsymbol{C}$ are constant (time-invariant) and if a partition of the state vector $\boldsymbol{x}$ (assumed m-dimensional) is available through measurement. Using the generic method presented in [10], the resulting observer typically has m manifolds and the SM motion is enforced at their intersection.

For the IM in particular, the stator currents are measured and they are also states of the model; then, it is common to use the current mismatches as the manifolds of the observer.

However, the state-space system corresponding to the IM is time-varying (since the speed ω_r appears in matrix $\boldsymbol{A}$). Therefore the generic SM design method cannot be directly used. In addition, for sensorless implementations, the speed ω_r also needs to be estimated.

The paper discusses the problem of state and speed estimation for the IM. In the first part, an SMO based on a single compound manifold is presented. It is shown that this observer does not fully converge; despite that, it yields the correct fluxes and a relatively accurate speed estimate. It was previously believed that this was a convergent observer and that its speed estimate was 100% accurate [10] – the theoretical analysis and the experimental implementation shown in the paper are both novel.

In the second part, the single-manifold design is augmented with additional feedback terms and this is transformed into a double-manifold SMO (DM SMO). The paper examines the properties of this design and shows that the estimates converge and the speed obtained is fully accurate.

Some considerations regarding the uniqueness of these observer designs are also presented.

The main contributions of the paper are: first, it corrects the analysis of the observer in [10] by showing that the current estimates do not converge and the resulting speed estimate is theoretically inaccurate; it also shows that, for the motor considered, this inaccuracy is small. It presents experimental waveforms and clarifies the behaviour of this observer – in a real implementation, this does not work. Then, the paper explains how to transform the single-manifold observer into a double-manifold design. The paper discusses the pairing of manifolds used by the double-manifold observer – it is shown that this observer design is unique. Finally, the paper presents a sensitivity analysis: it is found that this observer is rather sensitive to the value of the magnetising inductance; however, its estimates (especially the fluxes) are quite insensitive to the rotor resistance used.

2 Review of SM methods for the IM

In sensorless IM control, the problem is to estimate the speed, the flux magnitude and the rotor flux angle of the motor. From a theoretical point of view, if the motor parameters are known, several approaches can be used to obtain these variables.

From a practical point of view, there are two additional challenges: first, since the IM parameters vary with operating conditions (temperature, saturation, skin-effect), how to obtain accurate and reliable estimates in this case. Second, since some estimators employ complex or practically unreliable approaches (adaptation, parameter estimation, ideal integration), how to make the algorithms work well in a real implementation, in wide speed range, especially on digital signal processors with limited accuracy.

Generally, model-based estimation methods require accurate knowledge of the plant parameters. For the IM, both resistances depend on temperature (and this can vary by 100–150 °C from cold to hot). The magnetising inductance depends on the flux level in the machine – it is well-known that L_m saturates at high load.

To improve the estimation accuracy, the stator temperature can be measured using thermocouples; then, an updated value of R_S is used in the algorithm. The magnetising inductance can be approximately mapped to the operating conditions – the work in [24] gives a quadratic formula for L_m as a function of i_d; however, for a given motor, the coefficients of the quadratic must be obtained.

The SM methods for the IM in [15, 20] offer simultaneous estimation of the rotor fluxes, speed and rotor time constant. They are constructed based on the stationary frame model of the IM and assume that the speed and the rotor time constant vary slowly. The estimation is done by cascading a SMO with an adaptive linear observer: ω_r and η are obtained through adaptation (the mathematics is difficult and adaptation is always questionable under noise conditions). Note that under the same assumptions but with known fluxes, the model reference adaptive system (MRAS) method in [25] leads to singularity; then, only the speed (but not the rotor time constant) can be estimated. The practical accuracy of these methods depends heavily on the quality of the experimental setup (accuracy of current and voltage sensors, type of digital signal processor (DSP) used) and on the ability to make the observers work under pulse-width modulated (PWM) noise and dc offsets.

Some other SM methods only attempt to estimate the fluxes and the speed. The observer in [15] obtains the rotor fluxes by integration of the equivalent controls; flux estimation requires an accurate L_m but is insensitive to the rotor resistance. However, the accuracy of the speed estimate depends on R_r.

The methods in [16, 17] are similar in terms of model and approach, however, the insensitivity of the flux estimates to R_r is lost. The estimation/control method in [18] is looking to regulate the speed and the flux magnitude of the IM drive – the SM manifolds used are non-linear and depend on the speed and the load torque in order to satisfy the control objectives (as a result, the observer is more difficult to design).

The adaptive SMO in [19] designs the manifolds using the current mismatches; the speed is obtained using Lyapunov-based adaptation. The method offers good robustness to parameter variations. In [13], three sensorless SMOs and their parameter sensitivity analysis are presented. As expected, their accuracy depends on the values of L_m and R_r used.

Finally, note the sequential estimation approach proposed in [21, 22]. The idea is to first estimate the speed; then, to feed the speed estimate in a SMO (constructed on the stationary frame model of the IM) that obtains the motor fluxes. It is shown that, with a special gain design, even if the speed is inaccurate, the DFO estimated rotor flux angle is correct – thus, the field orientation of the drive is guaranteed. The same result is obtained in [23] where a time-varying observer that was designed using non-linear methods is shown. Finally, two flux/speed SMOs with compound manifolds are shown in [10, 20] – the work here was mainly inspired by them.

IET Electr. Power Appl., 2014, Vol. 8, Iss. 1, pp. 29–38
doi: 10.1049/iet-epa.2013.0192

3 Induction motor model

The model of the IM in the stationary reference frame with the notations from [10] is

$$\begin{cases} \dfrac{\mathrm{d}\lambda_\alpha}{\mathrm{d}t} = -\eta\lambda_\alpha - \omega_\mathrm{r}\lambda_\beta + \eta L_\mathrm{m} i_\alpha \\ \dfrac{\mathrm{d}\lambda_\beta}{\mathrm{d}t} = \omega_\mathrm{r}\lambda_\alpha - \eta\lambda_\beta + \eta L_\mathrm{m} i_\beta \\ \dfrac{\mathrm{d}i_\alpha}{\mathrm{d}t} = \eta\beta\lambda_\alpha + \omega_\mathrm{r}\beta\lambda_\beta - \gamma i_\alpha + \dfrac{1}{\sigma L_\mathrm{s}} v_\alpha \\ \dfrac{\mathrm{d}i_\beta}{\mathrm{d}t} = -\omega_\mathrm{r}\beta\lambda_\alpha + \eta\beta\lambda_\beta - \gamma i_\beta + \dfrac{1}{\sigma L_\mathrm{s}} v_\beta \end{cases} \tag{2}$$

Note that ω_r is the rotor electrical speed; this is related to the shaft speed as: $\omega_\mathrm{r} = n_\mathrm{p}\omega_\mathrm{r}^{\mathrm{mech}}$. The parameters σ, β, γ are defined as

$$\sigma = 1 - \frac{L_\mathrm{m}^2}{L_\mathrm{s}L_\mathrm{r}}, \quad \beta = \frac{L_\mathrm{m}}{\sigma L_\mathrm{s}L_\mathrm{r}}, \quad \gamma = \frac{1}{\sigma L_\mathrm{s}}\left(\frac{L_\mathrm{m}^2}{L_\mathrm{r}^2}R_\mathrm{r} + R_\mathrm{s}\right) \tag{3}$$

4 Single-manifold SMO for speed and state estimation of the IM

The equations of the single-manifold SMO (SM SMO) are

$$\begin{cases} \dfrac{\mathrm{d}\hat{\lambda}_\alpha}{\mathrm{d}t} = -\eta\hat{\lambda}_\alpha - \hat{\omega}_\mathrm{r}\hat{\lambda}_\beta + \eta L_\mathrm{m} i_\alpha \\ \dfrac{\mathrm{d}\hat{\lambda}_\beta}{\mathrm{d}t} = \hat{\omega}_\mathrm{r}\hat{\lambda}_\alpha - \eta\hat{\lambda}_\beta + \eta L_\mathrm{m} i_\beta \\ \dfrac{\mathrm{d}\hat{\imath}_\alpha}{\mathrm{d}t} = \eta\beta\hat{\lambda}_\alpha + \hat{\omega}_\mathrm{r}\beta\hat{\lambda}_\beta - \gamma i_\alpha + \dfrac{1}{\sigma L_\mathrm{s}} v_\alpha \\ \dfrac{\mathrm{d}\hat{\imath}_\beta}{\mathrm{d}t} = -\hat{\omega}_\mathrm{r}\beta\hat{\lambda}_\alpha + \eta\beta\hat{\lambda}_\beta - \gamma i_\beta + \dfrac{1}{\sigma L_\mathrm{s}} v_\beta \end{cases} \tag{4}$$

The speed estimate $\hat{\omega}_\mathrm{r}$ is of the form

$$\hat{\omega}_\mathrm{r} = \omega_0 \cdot \mathrm{sign}(s_1) \tag{5}$$

where ω_0 is a constant design gain. The manifold s_1 is

$$s_1 = \hat{\lambda}_\alpha\bar{\imath}_\beta - \hat{\lambda}_\beta\bar{\imath}_\alpha \tag{6}$$

In (4), the voltages v_α, v_β and currents i_α, i_β are measured quantities. The estimation mismatches are defined as: $\bar{\lambda}_\alpha = \hat{\lambda}_\alpha - \lambda_\alpha$, $\bar{\lambda}_\beta = \hat{\lambda}_\beta - \lambda_\beta$, $\bar{\imath}_\alpha = \hat{\imath}_\alpha - i_\alpha$, $\bar{\imath}_\beta = \hat{\imath}_\beta - i_\beta$.

By subtracting (2) from (4), the mismatch equations are

$$\begin{cases} \dfrac{\mathrm{d}\bar{\lambda}_\alpha}{\mathrm{d}t} = -\eta\bar{\lambda}_\alpha - \hat{\omega}_\mathrm{r}\hat{\lambda}_\beta + \omega_\mathrm{r}\lambda_\beta \\ \dfrac{\mathrm{d}\bar{\lambda}_\beta}{\mathrm{d}t} = \hat{\omega}_\mathrm{r}\bar{\lambda}_\alpha - \omega_\mathrm{r}\lambda_\alpha - \eta\bar{\lambda}_\beta \\ \dfrac{\mathrm{d}\bar{\imath}_\alpha}{\mathrm{d}t} = \eta\beta\bar{\lambda}_\alpha + \hat{\omega}_\mathrm{r}\beta\hat{\lambda}_\beta - \omega_\mathrm{r}\beta\lambda_\beta \\ \dfrac{\mathrm{d}\bar{\imath}_\beta}{\mathrm{d}t} = -\hat{\omega}_\mathrm{r}\beta\hat{\lambda}_\alpha + \omega_\mathrm{r}\beta\lambda_\alpha + \eta\beta\bar{\lambda}_\beta \end{cases} \tag{7}$$

To study the existence of the SM motion, s_1 is differentiated, this gives

$$\dot{s}_1 = \frac{\mathrm{d}\hat{\lambda}_\alpha}{\mathrm{d}t}\bar{\imath}_\beta + \hat{\lambda}_\alpha\frac{\mathrm{d}\bar{\imath}_\beta}{\mathrm{d}t} - \frac{\mathrm{d}\hat{\lambda}_\beta}{\mathrm{d}t}\bar{\imath}_\alpha - \hat{\lambda}_\beta\frac{\mathrm{d}\bar{\imath}_\alpha}{\mathrm{d}t} \tag{8}$$

In (8), replace the derivatives from (4) and (7), the result is

$$\begin{aligned} \dot{s}_1 = {} & -\eta\left(\hat{\lambda}_\alpha\bar{\imath}_\beta - \hat{\lambda}_\beta\bar{\imath}_\alpha\right) - \hat{\omega}_\mathrm{r}\left(\hat{\lambda}_\alpha\bar{\imath}_\alpha + \hat{\lambda}_\beta\bar{\imath}_\beta\right) \\ & + \eta L_\mathrm{m}\left(i_\alpha\bar{\imath}_\beta - i_\beta\bar{\imath}_\alpha\right) + \beta\omega_\mathrm{r}\left(\hat{\lambda}_\alpha\lambda_\alpha + \hat{\lambda}_\beta\lambda_\beta\right) \\ & + \beta\eta\left(\bar{\lambda}_\beta\hat{\lambda}_\alpha - \bar{\lambda}_\alpha\hat{\lambda}_\beta\right) - \beta\left(\hat{\lambda}_\alpha^2 + \hat{\lambda}_\beta^2\right)\hat{\omega}_\mathrm{r} \end{aligned} \tag{9}$$

Note that in (9), the speed estimate $\hat{\omega}_\mathrm{r}$ appears twice. The term $-\beta\left(\hat{\lambda}_\alpha^2 + \hat{\lambda}_\beta^2\right)\hat{\omega}_\mathrm{r}$ is very important. Assuming that this observer estimates the fluxes, $-\beta\left(\hat{\lambda}_\alpha^2 + \hat{\lambda}_\beta^2\right) = -\beta|\hat{\lambda}|^2 < 0$. Then, since this coefficient is reliable (non-zero and always negative), with high ω_0, the term $-\beta\left(\hat{\lambda}_\alpha^2 + \hat{\lambda}_\beta^2\right)\omega_0\,\mathrm{sign}(s_1)$ can be made as large as desired – this should enforce the SM motion on s_1.

On the other hand, the term $-\hat{\omega}_\mathrm{r}\left(\hat{\lambda}_\alpha\bar{\imath}_\alpha + \hat{\lambda}_\beta\bar{\imath}_\beta\right)$ may be undesirable since the presence of a second switching term on the right side of (9) could disturb the SM motion already in place. However, if the observer converges or if the current mismatches are small, the term $\left(\hat{\lambda}_\alpha\bar{\imath}_\alpha + \hat{\lambda}_\beta\bar{\imath}_\beta\right)$ should be zero or very small. By rewriting (9), this becomes

$$\begin{aligned} \dot{s}_1 = {} & f\left(\eta, \beta, \hat{\lambda}_\alpha, \hat{\lambda}_\beta, \bar{\imath}_\alpha, \bar{\imath}_\beta, \right) \\ & - \left[\beta\left(\hat{\lambda}_\alpha^2 + \hat{\lambda}_\beta^2\right) + \left(\hat{\lambda}_\alpha\bar{\imath}_\alpha + \hat{\lambda}_\beta\bar{\imath}_\beta\right)\right]\omega_0\,\mathrm{sign}(s_1) \end{aligned} \tag{10}$$

The function f is

$$\begin{aligned} f = {} & -\eta\left(\hat{\lambda}_\alpha\bar{\imath}_\beta - \hat{\lambda}_\beta\bar{\imath}_\alpha\right) + \eta L_\mathrm{m}\left(i_\alpha\bar{\imath}_\beta - i_\beta\bar{\imath}_\alpha\right) \\ & + \beta\omega_\mathrm{r}\left(\hat{\lambda}_\alpha\lambda_\alpha + \hat{\lambda}_\beta\lambda_\beta\right) + \beta\eta\left(\bar{\lambda}_\beta\hat{\lambda}_\alpha - \bar{\lambda}_\alpha\hat{\lambda}_\beta\right) \end{aligned} \tag{11}$$

Since f cannot tend to infinity (f has a finite upper estimate), if $\beta\left(\hat{\lambda}_\alpha^2 + \hat{\lambda}_\beta^2\right) + \left(\hat{\lambda}_\alpha\bar{\imath}_\alpha + \hat{\lambda}_\beta\bar{\imath}_\beta\right) > 0$, then, the SM motion can be enforced on manifold s_1.

If the design gain ω_0 is chosen to satisfy $\left[\beta\left(\hat{\lambda}_\alpha^2 + \hat{\lambda}_\beta^2\right) + \left(\hat{\lambda}_\alpha\bar{\imath}_\alpha + \hat{\lambda}_\beta\bar{\imath}_\beta\right)\right]\omega_0 > |f|$, the manifold and its derivative will have opposite signs ($s_1 \cdot \dot{s}_1 < 0$). As a result, the manifold is attractive and $s_1 \to 0$. After SM occurs, $s_1 = 0$ identically. It means that

$$\hat{\lambda}_\alpha\bar{\imath}_\beta - \hat{\lambda}_\beta\bar{\imath}_\alpha = 0 \tag{12}$$

From a theoretical point of view, $s_1 = 0$ does not necessarily imply that $\bar{\imath}_\alpha = 0$ and $\bar{\imath}_\beta = 0$. It will be shown immediately that (12) can be obtained with a set of non-zero fluxes and current mismatches.

Consider the vectors of the estimated flux and current mismatch shown in Fig. 1 (the angles θ and θ_1 are arbitrary). Then, their stationary reference frame components are

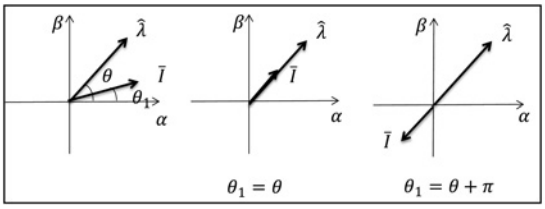

Fig. 1 *Flux and current mismatch vectors of the SM SMO*

$$\begin{cases} \hat{\lambda}_\alpha = \hat{\lambda} \cdot \cos(\theta) \\ \hat{\lambda}_\beta = \hat{\lambda} \cdot \sin(\theta) \end{cases} \quad \begin{cases} \bar{\imath}_\alpha = \bar{I} \cdot \cos(\theta_1) \\ \bar{\imath}_\beta = \bar{I} \cdot \sin(\theta_1) \end{cases} \tag{13}$$

Replacing (13) into (12), the expression of s_1 becomes

$$\begin{aligned} s_1 &= \hat{\lambda} \cdot \cos(\theta) \cdot \bar{I} \cdot \sin(\theta_1) - \hat{\lambda} \cdot \sin(\theta) \cdot \bar{I} \cdot \cos(\theta_1) \\ &= \hat{\lambda}\bar{I}\sin(\theta_1 - \theta) \end{aligned} \tag{14}$$

Based on (14), note that it is possible to have $s_1 = 0$ with $\bar{I} \neq 0$; for that, it is required that $\sin(\theta_1 - \theta) = 0$. This can happen if either $\theta_1 = \theta$ or if $\theta_1 = \theta + \pi$ (Fig. 1).

At this stage, the observer is simulated in order to study its behaviour. The IM drive is run in speed control mode: the motor is started towards a speed of 500 rpm and accelerates to 1000 rpm at $t = 0.5$ s. The load torque is 0.8 Nm. The observer is implemented with a 50 μs sampling time.

The simulations of this observer confirm the theoretical analysis. The SM motion occurs and s_1 tends to zero. The estimated fluxes of the observer tend to the real fluxes (note, however, that a theoretical proof of this cannot be done). The currents do not converge; therefore, the current mismatch vector is different from zero.

Fig. 2 shows the estimated against the real fluxes – they match. Manifold s_1 switches around zero; the current errors shown in Fig. 2 are non-zero and sinusoidal.

Fig. 3 shows the angle of $\bar{I}$ against the angle of $\hat{\lambda}$ and the speed estimate against the real speed. The angles are 180° out of phase (this corresponds to Fig. 1*c*).

This finding is one of the novelties in the paper. It was previously believed that this observer fully converges. The analysis in [10] assumes that, once SM occurs, the current mismatches are equal to zero and further concludes that the estimated speed tends to the real speed. This is inexact.

Note that since $\theta_1 = \theta + \pi$ (as shown by the simulations), the term $\hat{\lambda}_\alpha \bar{\imath}_\alpha + \hat{\lambda}_\beta \bar{\imath}_\beta$ becomes

$$\hat{\lambda}_\alpha \bar{\imath}_\alpha + \hat{\lambda}_\beta \bar{\imath}_\beta = -\hat{\lambda}\bar{I}\left[\sin^2(\theta) + \cos^2(\theta)\right] = -\hat{\lambda}\bar{I} \tag{15}$$

Then, working with (10) in the SM regime, the equivalent control is calculated by enforcing $s_1 = 0$ and $\dot{s}_1 = 0$. This is

$$\omega_{\mathrm{r,eq}} = \omega_{\mathrm{e}} \frac{\lambda_\alpha \hat{\lambda}_\alpha + \lambda_\beta \hat{\lambda}_\beta}{\hat{\lambda}^2 - [1/\beta]\hat{\lambda}\bar{I}} + \eta \frac{\hat{\lambda}_\alpha \bar{\lambda}_\beta - \hat{\lambda}_\beta \bar{\lambda}_\alpha}{\hat{\lambda}^2 - [1/\beta]\hat{\lambda}\bar{I}} \tag{16}$$

In practice, the equivalent would be obtained by low-pass filtering the switching manifold (5) – this represents the speed estimate of the observer. Based on (16), $\omega_{\mathrm{r,eq}} \to \omega_{\mathrm{r}}$ if the fluxes converge and if $\bar{\imath}_\alpha$, $\bar{\imath}_\beta$ are zero. Since the estimated fluxes tend to the real ones, the second term in (16) is equal to zero. The current mismatches $\bar{\imath}_\alpha$, $\bar{\imath}_\beta$ are non-zero (however, with a reasonable tuning for ω_0 they are relatively small).

For a typical IM, the magnetising inductance is much bigger than the leakage inductances. Then, σ. is small and β is large (e.g. $\sigma = 0.09$ and $\beta = 32.5$ for the motor considered). As a result, $1/\beta$ is small and the term $-[1/\beta]\hat{\lambda}\bar{I}$ in the denominator of (16) is much smaller than $\hat{\lambda}^2$. Therefore the equivalent control $\omega_{\mathrm{r,eq}}$ given by (16) is quite close to the real speed of the motor (Fig. 3).

Additional simulations were attempted with smaller values of β in order to determine whether this is a major factor in the accuracy of the speed estimate (16). It was found that β has a small influence.

In conclusion, the observer based on the single compound manifold s_1 offers a simple design and has interesting properties. Although it does not fully converge, it yields accurate fluxes and a sufficiently accurate speed estimate. Its experimental reliability remains to be seen.

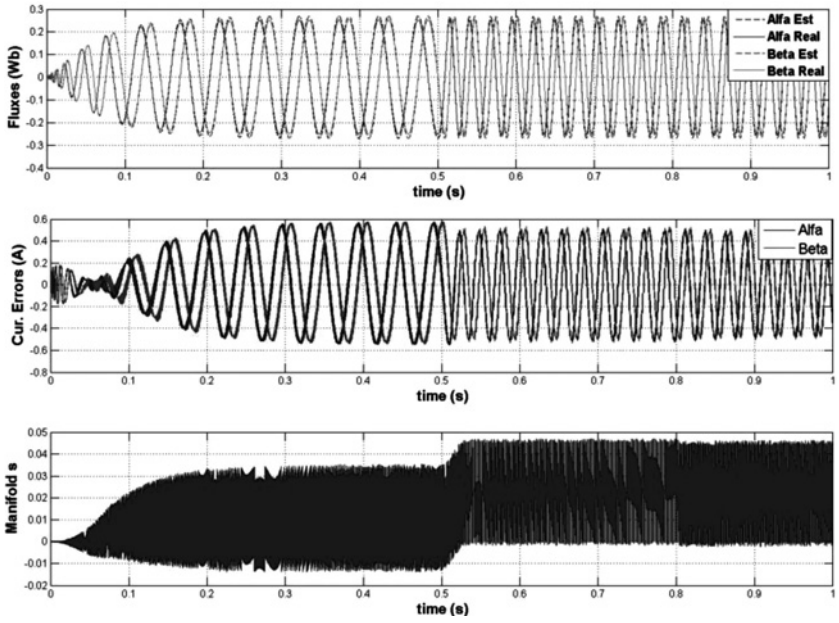

Fig. 2 *Fluxes, current errors and manifold of the SMO*

IET Electr. Power Appl., 2014, Vol. 8, Iss. 1, pp. 29–38
doi: 10.1049/iet-epa.2013.0192

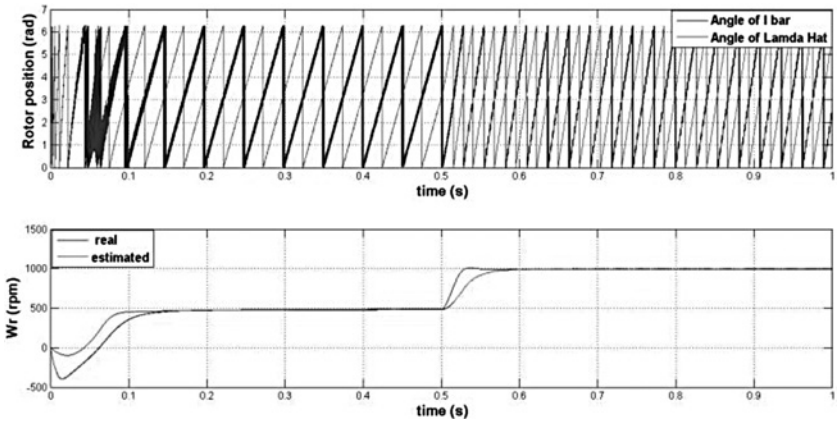

Fig. 3 *Angle of current mismatches against angle of the estimated fluxes and estimated against real speed*

Note that three other manifolds similar to (6) can be obtained by combining the fluxes $\hat{\lambda}_\alpha$, $\hat{\lambda}_\beta$ with $\bar{\imath}_\alpha$, $\bar{\imath}_\beta$. However, s_1 is the only manifold that leads to a valid observer. We have verified analytically and by simulation that the design based on s_1 is unique.

5 DM SMO for speed and state estimation of the IM

The proposed DM SMO is obtained by augmenting the design given by (4) with additional feedback terms – these are also switching terms. The objective is to obtain an observer that enforces the SM motion at the intersection of two manifolds. If SM occurs and the manifolds are simultaneously equal to zero, this should improve the estimation properties of the SM SMO.

The manifolds chosen are

$$\begin{cases} s_1 = \hat{\lambda}_\alpha \bar{\imath}_\beta - \hat{\lambda}_\beta \bar{\imath}_\alpha \\ s_2 = \hat{\lambda}_\alpha \bar{\imath}_\alpha + \hat{\lambda}_\beta \bar{\imath}_\beta \end{cases} \tag{17}$$

If SM could be enforced on these manifolds, then, $s_1 = 0$, $s_2 = 0$. This is equivalent to

$$\begin{bmatrix} -\hat{\lambda}_\beta & \hat{\lambda}_\alpha \\ \hat{\lambda}_\alpha & \hat{\lambda}_\beta \end{bmatrix} \begin{bmatrix} \bar{\imath}_\alpha \\ \bar{\imath}_\beta \end{bmatrix} = \begin{bmatrix} 0 \\ 0 \end{bmatrix} \tag{18}$$

Since $\det(\mathbf{\Lambda}) = -\left(\hat{\lambda}_\alpha^2 + \hat{\lambda}_\beta^2\right) \neq 0$. (assuming that the fluxes converge), system (18) has unique solution: $\bar{\imath}_\alpha = 0$, $\bar{\imath}_\beta = 0$. Therefore the current estimates of this observer would be guaranteed to converge.

Note that, manifold s_2 is the only viable pairing option for s_1 that leads to a non-zero determinant. Since the SM SMO based on s_1 is unique, it follows that the DM SMO based on the pair s_1, s_2 is also unique. The equations of the proposed DM SMO are

$$\begin{cases} \dfrac{\mathrm{d}\hat{\lambda}_\alpha}{\mathrm{d}t} = -\eta\hat{\lambda}_\alpha - \hat{\omega}_\mathrm{r}\hat{\lambda}_\beta + \eta L_\mathrm{m} i_\alpha \\ \dfrac{\mathrm{d}\hat{\lambda}_\beta}{\mathrm{d}t} = \hat{\omega}_\mathrm{r}\hat{\lambda}_\alpha - \eta\hat{\lambda}_\beta + \eta L_\mathrm{m} i_\beta \\ \dfrac{\mathrm{d}\hat{\imath}_\alpha}{\mathrm{d}t} = \eta\beta\hat{\lambda}_\alpha + \hat{\omega}_\mathrm{r}\beta\hat{\lambda}_\beta - \gamma i_\alpha + \dfrac{1}{\sigma L_\mathrm{S}} v_\alpha - k\hat{\lambda}_\alpha u_2 \\ \dfrac{\mathrm{d}\hat{\imath}_\beta}{\mathrm{d}t} = -\hat{\omega}_\mathrm{r}\beta\hat{\lambda}_\alpha + \eta\beta\hat{\lambda}_\beta - \gamma i_\beta + \dfrac{1}{\sigma L_\mathrm{s}} v_\beta - k\hat{\lambda}_\beta u_2 \end{cases} \tag{19}$$

where k is a design parameter. The switching terms are

$$\begin{cases} \hat{\omega}_\mathrm{r} = \omega_0 \cdot \mathrm{sign}(s_1) \\ u_2 = M \cdot \mathrm{sign}(s_2) \end{cases} \tag{20}$$

In (20), ω_0 and M are design gains. Note that this is similar to the observer in [20]. After subtraction, the mismatches are

$$\begin{cases} \dfrac{\mathrm{d}\bar{\lambda}_\alpha}{\mathrm{d}t} = -\eta\bar{\lambda}_\alpha - \hat{\omega}_\mathrm{r}\hat{\lambda}_\beta + \omega_\mathrm{r}\lambda_\beta \\ \dfrac{\mathrm{d}\bar{\lambda}_\beta}{\mathrm{d}t} = \hat{\omega}_\mathrm{r}\hat{\lambda}_\alpha - \omega_\mathrm{r}\lambda_\alpha - \eta\bar{\lambda}_\beta \\ \dfrac{\mathrm{d}\bar{\imath}_\alpha}{\mathrm{d}t} = \eta\beta\bar{\lambda}_\alpha + \hat{\omega}_\mathrm{r}\beta\hat{\lambda}_\beta - \omega_\mathrm{r}\beta\lambda_\beta - k\hat{\lambda}_\alpha u_2 \\ \dfrac{\mathrm{d}\bar{\imath}_\beta}{\mathrm{d}t} = -\hat{\omega}_\mathrm{r}\beta\hat{\lambda}_\alpha + \omega_\mathrm{r}\beta\lambda_\alpha + \eta\beta\bar{\lambda}_\beta - k\hat{\lambda}_\beta u_2 \end{cases} \tag{21}$$

To examine whether SM occurs, the two manifolds are differentiated and the derivatives are replaced. The derivative of s_1 is

$$\begin{aligned} \dot{s}_1 = &-\eta\left(\hat{\lambda}_\alpha\bar{\imath}_\beta - \hat{\lambda}_\beta\bar{\imath}_\alpha\right) - \hat{\omega}_\mathrm{r}\left(\hat{\lambda}_\alpha\bar{\imath}_\alpha + \hat{\lambda}_\beta\bar{\imath}_\beta\right) \\ &+ \eta L_\mathrm{m}\left(i_\alpha\bar{\imath}_\beta + i_\beta\bar{\imath}_\alpha\right) + \beta\omega_\mathrm{r}\left(\hat{\lambda}_\alpha\lambda_\alpha + \hat{\lambda}_\beta\lambda_\beta\right) \\ &+ \beta\eta\left(\bar{\lambda}_\beta\hat{\lambda}_\alpha - \bar{\lambda}_\alpha\hat{\lambda}_\beta\right) - \beta\left(\hat{\lambda}_\alpha^2 + \hat{\lambda}_\beta^2\right)\hat{\omega}_\mathrm{r} \end{aligned} \tag{22}$$

The derivative of s_2 is

$$\begin{aligned} \dot{s}_2 = &-\eta\left(\hat{\lambda}_\alpha\bar{\imath}_\alpha + \hat{\lambda}_\beta\bar{\imath}_\beta\right) + \hat{\omega}_\mathrm{r}\left(\hat{\lambda}_\alpha\bar{\imath}_\beta - \hat{\lambda}_\beta\bar{\imath}_\alpha\right) \\ &+ \eta L_\mathrm{m}\left(i_\alpha\bar{\imath}_\alpha + i_\beta\bar{\imath}_\beta\right) + \beta\eta\left(\bar{\lambda}_\alpha\hat{\lambda}_\alpha + \bar{\lambda}_\beta\hat{\lambda}_\beta\right) \\ &- \beta\omega_\mathrm{r}\left(\hat{\lambda}_\alpha\lambda_\beta - \hat{\lambda}_\beta\lambda_\alpha\right) - k\left(\hat{\lambda}_\alpha^2 + \hat{\lambda}_\beta^2\right)u_2 \end{aligned} \tag{23}$$

Note that the switching term $u_2$does not appear in (22). The above expressions can be rewritten as

$$\begin{cases} \dot{s}_1 = f_1 - \beta\left(\hat{\lambda}_\alpha^2 + \hat{\lambda}_\beta^2\right) \cdot \omega_0 \cdot \mathrm{sign}(s_1) \\ \dot{s}_2 = f_2 - k\left(\hat{\lambda}_\alpha^2 + \hat{\lambda}_\beta^2\right) \cdot M \cdot \mathrm{sign}(s_2) \end{cases} \tag{24}$$

By inspecting expressions (22) and (23), the functions f_1, f_2 are a combination of the estimates, the observer mismatches

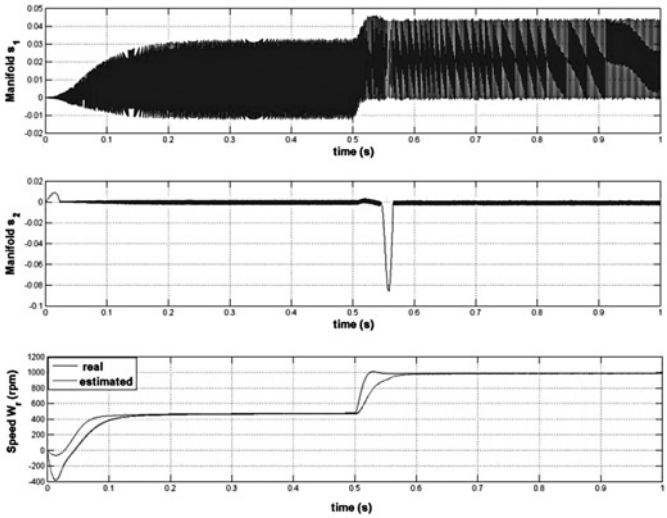

Fig. 4 *Manifolds s_1, s_2 and the speed estimate of the DM SMO*

and also involve the speed and the motor parameters. If the estimates are finite, both functions have an upper estimate (they do not tend to infinity). Based on (24), if the gains ω_0 and M are chosen high enough, assuming that $\hat{\lambda}_\alpha^2 + \hat{\lambda}_\beta^2 \neq 0$, the switching terms on the right side of (24) will be such that

$$\begin{cases} \beta\left(\hat{\lambda}_\alpha^2 + \hat{\lambda}_\beta^2\right) \cdot \omega_0 > |f_1| \\ k\left(\hat{\lambda}_\alpha^2 + \hat{\lambda}_\beta^2\right) \cdot M > |f_2| \end{cases} \tag{25}$$

Then, s_1 and $\dot{s}_1$ have opposite signs; the same for s_2 and $\dot{s}_2$. As a result, the manifolds are attractive and $s_1 \to 0$, $s_2 \to 0$; then, SM will occur at the intersection of these manifolds. Once SM starts, we can assume that $s_1 = 0$, $s_2 = 0$ identically. Note that ω_0 and M are the only design gains of the observer (k can be incorporated into M) and the only condition that they need to satisfy is (25).

Unlike in MRAS-type estimators, for the proposed SMO it does not matter whether the drive runs in motoring or regeneration. The value and sign of ω_r (positive or negative) affects the magnitudes of f_1 and f_2. However, it is only required to know the maximum of these functions in order to design appropriate (high enough) gains that satisfy (25). Then, SM occurs, the current mismatches are zero and the flux estimates are obtained. Once the flux components are available, the flux angle is computed and the field-oriented control algorithm can be executed.

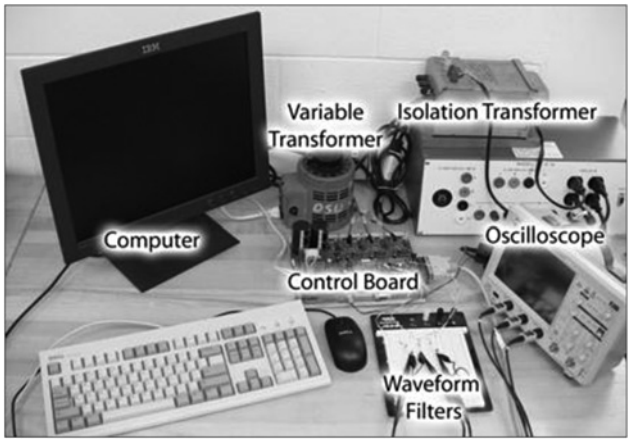

Fig. 5 *Experimental setup*

The simulations of this observer are done under the same conditions as before. Fig. 4 shows the manifolds s_1, s_2 – they both tend to zero since SM occurs. The estimated fluxes tend to the real fluxes. The current estimates converge and the mismatches $\bar{\imath}_\alpha$, $\bar{\imath}_\beta$ tend to zero as per (18).

Working with the expression of s_1 during the SM regime, since $\bar{\imath}_\alpha = 0$, $\bar{\imath}_\beta = 0$, it follows that $\left(\hat{\lambda}_\alpha \bar{\imath}_\alpha + \hat{\lambda}_\beta \bar{\imath}_\beta\right) = 0$. As a result, there is only one term that depends on $\hat{\omega}_r$ in (22). With $s_1 = 0$ and $\dot{s}_1 = 0$, the equivalent control is obtained as

$$\omega_{r,eq} = \omega_r \frac{\lambda_\alpha \hat{\lambda}_\alpha + \lambda_\beta \hat{\lambda}_\beta}{\hat{\lambda}^2} + \eta \frac{\hat{\lambda}_\alpha \bar{\lambda}_\beta - \hat{\lambda}_\beta \bar{\lambda}_\alpha}{\hat{\lambda}^2} \tag{26}$$

Since the fluxes converge, the second term in (26) is 0 and the other term is 1. Therefore it is clear that $\omega_{r,eq} \to \omega_r$ (Fig. 4). The estimated speed tends to the real speed with a rate that depends on the rate of decay of manifold s_1. If $\bar{\lambda}_\alpha$ and $\bar{\lambda}_\beta$ are always zero and the SM motion on s_1 is not perturbed, $\omega_{r,eq}$ matches ω_r exactly. Note that this is the speed estimate of the method and is obtained by low-pass filtering the switching manifold s_1. Unlike the approximation (16) of the SM SMO, the speed estimate of the DM SMO is fully accurate.

Regarding the design of ω_0, note that, according to (25), it is required that $\beta\left(\hat{\lambda}_\alpha^2 + \hat{\lambda}_\beta^2\right) \cdot \omega_0 > |f_1|$. Then, for a drive that operates at variable flux level and variable speed (f_1 depends on speed), an adequate value for ω_0 can be found. Another necessary condition is $\omega_0 > \omega_r$. Since the speed estimate is obtained by filtering the switching term $\omega_0 \cdot \text{sign}(s_1)$, if the drive operates at high speed, ω_0 should also be proportionally high. However, if the same drive is now required to operate at low speed, the high value of ω_0 is problematic (produces chattering) and should be reduced. In fact, the observer performs best with a speed adaptive value for ω_0 that satisfies the conditions above. This idea was explored for other SMOs (e.g. [28]).

Also, note that the SM motion of s_1 is free of the switching term $M \cdot \text{sign}(s_2)$. However, the motion equation of s_2 contains the term $\omega_0 \cdot \text{sign}(s_1)$ (this term, for example, acts

doi: 10.1049/iet-epa.2013.0192

as a disturbance when the observer runs under improper parameters). Then, ω_0 should not be overdesigned (e.g. if the drive runs at 300 rad/s, it is detrimental to use a value of ω_0 more than 1.5–2 times higher than that).

6 Experimental results

The experimental setup consists of a Dayton 2N863M three-phase squirrel cage motor (see specifications in Table 1), a Texas Instruments TMS320F2812 DSP, and a Spectrum Digital metal-oxide semiconductor field-effect transisitor inverter (Fig. 5). An autotransformer was used to adjust the dc bus voltage and an isolation transformer was used to protect the hardware. The waveforms are captured with a 200 MHz LeCroy oscilloscope.

The control algorithm was implemented in 32 bit fixed point math using a single interrupt. The sampling time is 66 μs (the inverter switches at 15 kHz). The output waveforms are generated using the second PWM state machine of the TMS320F2812 chip. These signals are low-pass filtered with RC circuits and are captured using the scope channels (three signals can be captured at one time). The phase currents are measured with resistors mounted on the lower legs of the inverter. The motor voltages are computed from the measured dc bus voltage and the PWM duty cycles.

Since the motor used in the experimental setup does not have an encoder, an estimate of the IM speed is obtained from the slip (27) – this will be compared with the speed obtained from the proposed methods.

$$\hat{\omega}_r = \omega_e - \frac{L_m}{T_r}\frac{1}{\hat{\lambda}_r^2}\left(\hat{\lambda}_\alpha i_\beta - \hat{\lambda}_\beta i_\alpha\right) \tag{27}$$

Also, since the fluxes cannot be measured, the estimated fluxes of the observer are compared with the fluxes obtained from the voltage model observer (VMO) corresponding to the method in [26].

In the experiments shown, the IM drive runs in field-oriented speed control mode and the observer is validated. The base quantities of the experimental setup are: $V_B = 179.7$ V (peak); $I_B = 3.75$ A (peak); $\omega_B = 377$ rad/s; $\lambda_B = L_m I_B = 1.1137$ Wb.

The DM SMO is implemented first. System (19) is discretised using Euler's method; the per-unit equations are

$$\begin{cases} \hat{\lambda}_{\alpha,k+1} = A_1\hat{\lambda}_{\alpha,k} - A_2\hat{\omega}_r\hat{\lambda}_{\beta,k} + A_3 i_\alpha \\ \hat{\lambda}_{\beta,k+1} = A_2\hat{\omega}_r\hat{\lambda}_{\alpha,k} + A_1\hat{\lambda}_{\beta,k} + A_3 i_\beta \\ \hat{\imath}_{\alpha,k+1} = \hat{\imath}_{\alpha,k} + A_4\hat{\lambda}_{\alpha,k} + A_5\hat{\omega}_r\hat{\lambda}_{\beta,k} - A_6 i_\alpha + A_7 v_\alpha - kA_8\hat{\lambda}_{\alpha,k}u_2 \\ \hat{\imath}_{\beta,k+1} = \hat{\imath}_{\beta,k} - A_5\hat{\omega}_r\hat{\lambda}_{\alpha,k} + A_4\hat{\lambda}_{\beta,k} - A_6 i_\beta + A_7 v_\beta - kA_8\hat{\lambda}_{\beta,k}u_2 \end{cases} \tag{28}$$

Table 1 IM specifications and parameters

rating	¼ hp	pole #	4
speed	1732 rpm	voltage	220 V
R_s			10.9 Ω
L_{ls}, L_{lr}			0.015 H
L_m			0.30 H
R_r			5.57 Ω

The constants A_1 through A_8 are: $A_1 = 1 - \eta T_S$; $A_2 = \omega_B T_S$; $A_3 = \eta L_m T_S(I_B/\lambda_B)$; $A_4 = \eta\beta T_S(\lambda_B/I_B)$; $A_5 = \beta T_S\omega_B(\lambda_B/I_B)$; $A_6 = \gamma T_S$; $A_7 = (T_S/\sigma L_S)(V_B/I_B)$; $A_8 = \lambda_B/I_B$.

Note that k is a design gain. With $k = 0$, the switching term u_2 disappears from the equations of the currents in (19); then, the DM SMO becomes the SM SMO. Therefore a single software implementation allows investigation of both observers presented in the paper.

In the experiment, the motor runs in speed control mode at about 800 rpm with a load of 0.2 Nm. The observer gains are $\omega_0 = 7$ pu, $M = 3$ pu, $k = 1$. The SMO is implemented using the well-known linear approximation of the sign function in [10]; the threshold is equal to 0.05 pu.

Fig. 6 shows the currents, fluxes and flux angle of the DM SMO. The estimated current matches the real current quite well. As expected from (18), $\bar{\imath}_\alpha = 0$ ($\bar{\imath}_\beta = 0$ also). The β-axis waveforms are similar and are omitted. The estimated fluxes are shown in comparison with the fluxes obtained from the VMO in [26] – they match in both magnitude and phase. Therefore the estimated rotor flux angles shown also correspond.

Fig. 7 shows the accuracy of the speed estimate of the DM SMO. The IM drive runs in vector control mode and the motor goes through acceleration, deceleration and speed reversal with 0.2 Nm load.

The speed estimate of the DM SMO is shown along the speed estimate obtained with (27). Both signals have been filtered with 15 rad/s low-pass filters. It can be seen that the

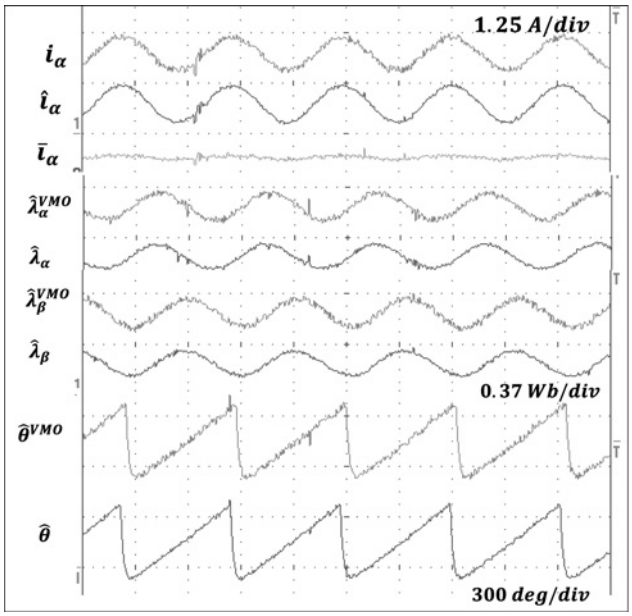

Fig. 6 *Currents, fluxes and the rotor flux angle of the DM SMO*

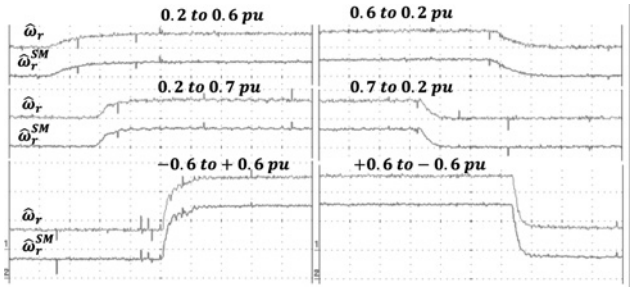

Fig. 7 *Accuracy of the speed estimate of the DM SMO*

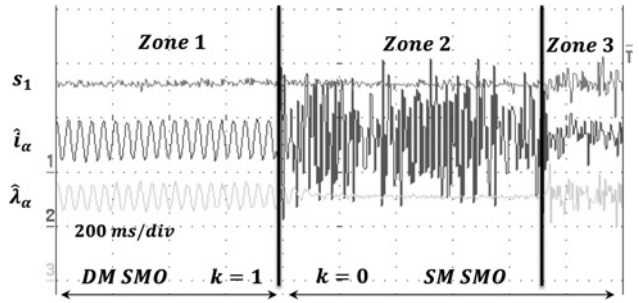

Fig. 8 *Manifold s_1, estimated current and estimated flux at transition from DM SMO to SM SMO*

speed estimate of the observer is fairly accurate both during transient and at steady state.

Since the SMOs are constructed based on the motor model in the stationary reference frame, the paper shows the plots of the stationary frame ($\alpha - \beta$) currents and fluxes. The plots in Fig. 6 show that estimated fluxes of the DM SMO are accurate – in conclusion, this validates the theoretical development and the simulations.

Fig. 8 shows the transition from the DM SMO to the SM SMO – for that, the gain k in (28) is changed from 1 to 0. Fig. 8 shows three zones associated with this transition; note that the SM SMO does not behave well.

In Zone I, the DM SMO runs at steady state, the estimated current, the estimated flux and s_1 are shown. They all look as expected and $s_1 = 0$.

At transition, $k = 0$, therefore the SM term u_2 vanishes and the resulting observer is SM SMO. It can be seen that $\hat{i}_\alpha$ starts having high magnitude whereas $\hat{\lambda}_\alpha$ tends to zero. They are both unusable. Note that in Zone II, $s_1 = 0$ still; however, this is not because the SM motion is enforced on s_1, but rather because both $\hat{\lambda}_\alpha$ and $\hat{\lambda}_\beta$ are zero. With that, the term $\beta\left(\hat{\lambda}_\alpha^2 + \hat{\lambda}_\beta^2\right) + \left(\hat{\lambda}_\alpha \bar{i}_\alpha + \hat{\lambda}_\beta \bar{i}_\beta\right)$ in (10) should also be zero. Under these conditions, the SM motion does not exist.

Finally, in Zone III, the current estimate, the flux estimate and the manifold s_1 all collapse. The observer triggers on noise and the waveforms are pretty much random.

The experiment shows that the SM SMO is not a reliable method for state and speed estimation of the IM drive. The theoretical analysis of the SM SMO was based on the assumption that the fluxes converge. It can be seen that, under experimental conditions, this is not the case.

Several other values for the gains were tried; it was also tried to start the drive using the SM SMO; however, this observer has not performed. However, note that this provides a useful starting point for the development of the DM SMO.

Fig. 9 shows the currents, fluxes and the estimated rotor flux angle during a -0.3 to 0.3 p.u. speed reversal at 0.1 Nm load. The estimated fluxes and current i_d shows some oscillation as a result of the zero-crossing. Note that the fluxes are still useable and are not affected by the regeneration mode of the drive.

The DM SMO was confirmed to work and appears to be accurate. Experimentally, it was seen that if the gains ω_0 and M are too small, the SM motion does not occur; however, the observer will not recover even if the gains are increased. Also, the double switching action is problematic if the dc offsets and noise levels are high – in this case, the DM SMO is less reliable than an observer with continuous feedback.

Fig. 10 shows more experimental results of the drive–observer system at acceleration (0.2–0.7 pu) and deceleration (0.7–0.2 pu). The load torque is ~ 0.2 Nm. Fig. 10*a* shows the currents i_d, i_q and the flux magnitude $\hat{\lambda}_r$. Fig. 10*b* shows the flux components $\hat{\lambda}_\alpha$, $\hat{\lambda}_\beta$. Fig. 10*c* shows the plots of $\hat{\lambda}_\alpha$ as a function of $\hat{\lambda}_\beta$. At steady state, this is a perfect circle; at transient deceleration, the circle is slightly distorted and then it recovers.

7 Sensitivity analysis

This section investigates the sensitivity of the DM SMO to the variation of the IM parameters. The variation of the rotor resistance R_r and of the magnetising inductance L_m is considered. The variation of R_s is not considered (if needed, R_s can be estimated using stator-mounted thermistors). The observer is implemented using the rated parameters while the plant is detuned: R_r is increased up to double the rated value; L_m is reduced to half its rated value (this corresponds to a practical situation).

The motor runs at 1000 rpm with 0.8 Nm of load. Fig. 11 shows the flux angle estimation error $\Delta\theta = \hat{\theta} - \theta$, the speed

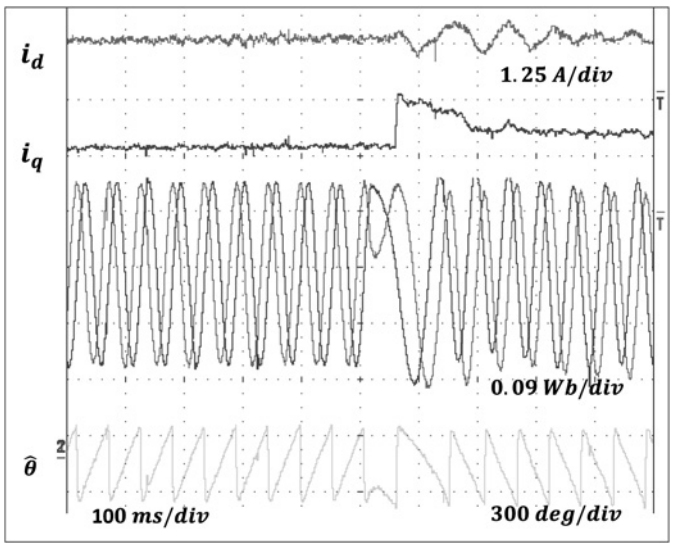

Fig. 9 *Currents, fluxes and the rotor flux angle of the DM SMO during speed reversal*

IET Electr. Power Appl., 2014, Vol. 8, Iss. 1, pp. 29–38
doi: 10.1049/iet-epa.2013.0192

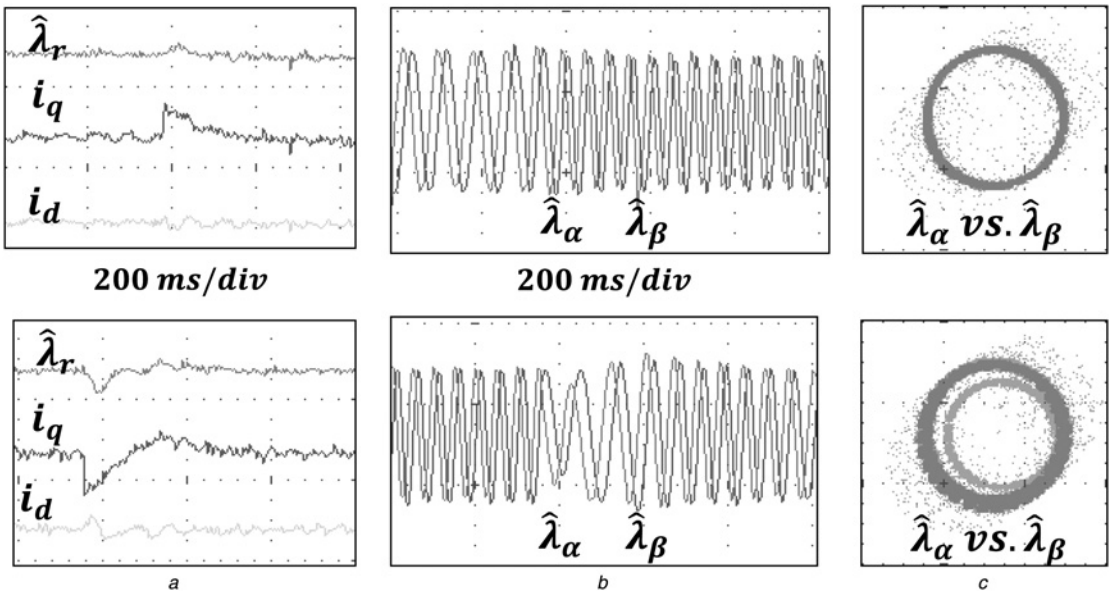

Fig. 10 *Acceleration/deceleration*

a Currents and flux magnitude
b Stationary frame fluxes
c $\hat{\lambda}_\alpha$ as a function of $\hat{\lambda}_\beta$

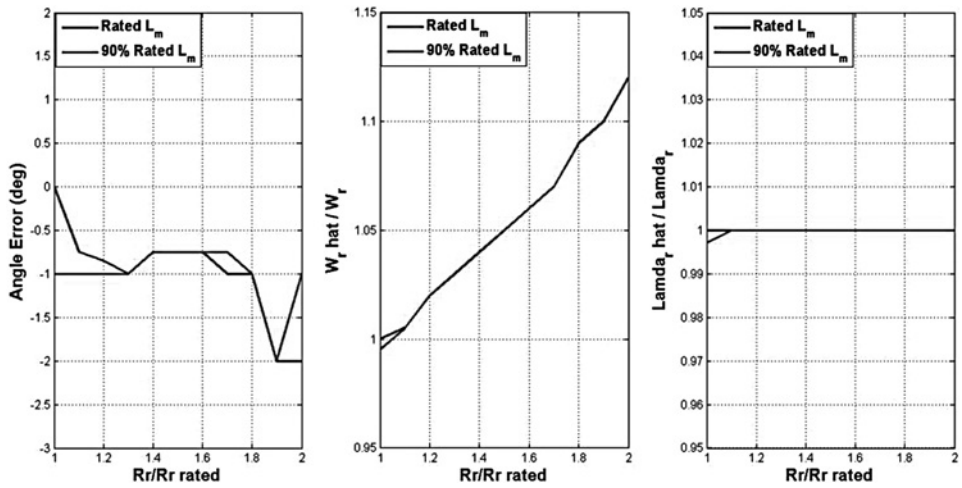

Fig. 11 *Angle, speed and flux errors of the DM SMO under improper parameters*

error $\Delta\omega_r = (\hat{\omega}_r/\omega_r)$ and the flux magnitude error $\Delta\lambda_r = (\hat{\lambda}_r/\lambda_r)$ at steady state.

Simulations show that the observer is rather sensitive to L_m and is quite insensitive to R_r. At the start of the investigation, the SM gains ω_0 and M are tuned such that the observer works well with rated parameters ($\omega_0 = 240$ and $M = 40$). Then, the IM parameters are detuned. It is seen that if L_m saturates down to ~25% of its rated value, the observer performs very well and the estimates are accurate. However, beyond that range, the SM motion is perturbed and the estimates are not reliable. Therefore, it is required to use a rather precise value of L_m. Note that a quadratic mapping of this as a function of i_d was proposed in [27].

Simulations show that the observer is quite insensitive to the variation of R_r. If L_m is in the 25% accuracy range, a variation of R_r of up to 100% produces very little drift in the estimates.

Fig. 11 shows the errors: the angle error is very small (2°), the magnitude error is virtually inexistent and the speed error is no higher than 12%.

To summarise: if the magnetising inductance used by the observer is within 25% of the real L_m, the rotor resistance of the motor can be as high as double the rated R_r (used by the observer); then, the angle error is within 2°, the flux magnitude error is zero and the speed error is within 12%. These properties are not necessarily unique but are consistent with those of a good observer.

Generally, the dependence of the speed estimate to the rotor resistance is typical of sensorless estimators – note that this corresponds to (27), which follows the equation of the IM in the synchronous reference frame. Regarding the insensitivity of the fluxes to R_r, there are other estimators that exhibit this property, for example, the well-known VMO.

8 Conclusions

The paper discusses the problem of speed and state estimation for the IM and presents a single- and a double-manifold SMO

for speed and state estimation. Both observers are designed using the stationary reference frame model of the motor and use special manifolds. It is shown that, theoretically, the single-manifold observer does not fully converge; despite this, it estimates the fluxes and yields a relatively accurate speed estimate. Its experimental implementation shows that this method is not viable – the observer does not work at all. The double-manifold observer is obtained as an extension of the first design by adding extra feedback terms. Since the SM motion is enforced at the intersection of the manifolds, the currents are guaranteed to converge. The estimated fluxes and speed are accurate. It is found that, under improper parameters, this observer is sensitive to the variation of the magnetising inductance and is quite robust to the value of the rotor resistance. The theoretical developments are confirmed by the experimental results – the method yields fairly accurate estimates.

9 References

1 Hinkkanen, M.: 'Analysis and design of full order flux observers for sensorless induction motors', *IEEE Trans. Ind. Electron.*, 2004, **51**, (5), pp. 1033–1040
2 Kim, J.H., Choi, J.W., Sul, S.K.: 'Novel rotor flux observer using observer characteristic function in complex vector space for field oriented induction motor drives', *IEEE Trans. Ind. Appl.*, 2002, **38**, pp. 1334–1343
3 Lascu, C., Boldea, I., Blaabjerg, F.: 'Comparative study of adaptive and inherently sensorless observers for variable speed induction motor drives', *IEEE Trans. Ind. Electron.*, 2006, **53**, (1), pp. 57–65
4 Vaclavek, P., Blaha, P.: 'Lyapunov function based flux and speed observer for AC induction motor sensorless control and parameter estimation', *IEEE Trans. Ind. Electron.*, 2006, **53**, (1), pp. 138–145
5 Harnefors, L., Hinkkanen, M.: 'Complete stability of reduced order and full order observers for IM drives', *IEEE Trans. Ind. Electron.*, 2008, **55**, pp. 1319–1329
6 Cirrincione, M., Pucci, M., Cirrincione, G., Capolino, G.A.: 'Sensorless control of induction motors by reduced order observer with MCA-EXIN based adaptive speed estimation', *IEEE Trans. Ind. Electron.*, 2007, **54**, pp. 150–166
7 Alonge, F., D'Ippolito, F., Giardina, G., Scaffidi, T.: 'Design and low cost implementation of an optimally robust reduced order rotor flux observer for induction motor control', *IEEE Trans. Ind. Electron.*, 2007, **54**, pp. 3205–3216
8 Hinkkanen, M., Harnefors, L., Luomi, J.: 'Reduced-order flux observers with stator resistance adaptation for speed sensorless induction motor drives'. IEEE Energy Conversion and Exposition, San Jose, CA, 2009, pp. 155–162
9 Montanari, M., Peresada, S.M., Rossi, C., Tilli, A.: 'Speed sensorless control of induction motors based on a reduced-order adaptive observer', *IEEE Trans. Control Syst. Technol.*, 2007, **15**, pp. 1049–1064
10 Utkin, V.I., Guldner, J.G., Shi, J.: 'Sliding mode control in electromechanical systems' (Taylor and Francis, New York, 1999, 1st edn)
11 Yan, Z., Utkin, V.I.: 'Sliding mode observers for electric machines – an overview'. Twenty-eighth Annual Conf. on Industrial Electronics Society (IECON '02), Sevilla, Spain, 2002, vol. 3, pp. 1842–1847
12 Yan, Z., Jin, C., Utkin, V.I.: 'Sensorless sliding-mode control of induction motors', *IEEE Trans. Ind. Electron.*, 2000, **47**, pp. 1286–1297
13 Lascu, C., Boldea, I., Blaabjerg, F.: 'A class of speed-sensorless sliding-mode observers for high-performance induction motor drives', *IEEE Trans. Ind. Electron.*, 2009, **56**, (9), pp. 3394–3403
14 Li, J., Xu, L., Zhang, Z.: 'An adaptive sliding mode observer for induction motor sensorless speed control', *IEEE Trans. Ind. Appl.*, 2005, **41**, pp. 1039–1046
15 Derdiyok, A., Yan, Z., Guven, M., Utkin, V.I.: 'A sliding mode speed and rotor time constant observer for induction machines'. The 27th Annual Conf. on IEEE Industrial Electronics Society, 2001, pp. 1400–1404
16 Rehman, H., Derdiyok, A., Guven, M.K., Xu, L.: 'A new current model flux observer for wide speed range sensorless control of an induction machine', *IEEE Trans. Power Electron.*, 2002, **7**, (6), pp. 1041–1048
17 Zhang, Z., Xu, H., Xu, L., Heilman, L.E.: 'Sensorless direct field-oriented control of three-phase induction motors based on sliding mode for washing machine drive applications', *IEEE Trans. Ind. Appl.*, 2006, **42**, (3), pp. 694–701
18 Benchaib, A., Rachid, A., Audrezet, E., Tadjine, M.: 'Real-time sliding mode observer and control of an induction motor', *IEEE Trans. Ind. Electron.*, 1999, **46**, (1), pp. 128–138
19 Tursini, M., Petrella, R., Parasiliti, F.: 'Adaptive sliding mode observer for speed sensorless control of induction motors', *IEEE Trans. Ind. Appl.*, 2000, **36**, (5), pp. 1380–1387
20 Rao, S., Buss, M., Utkin, V.I.: 'Simultaneous state and parameter estimation in induction motors using first and second order sliding modes', *IEEE Trans. Ind. Electron.*, 2009, **56**, (9), pp. 3369–3376
21 Korlinchak, C., Comanescu, M.: 'Robust sensorless sliding mode flux observer with speed estimate for induction motor drives', *Electr. Power Compon. Syst. J.*, 2012, **40**, (9), pp. 1030–1049
22 Comanescu, M.: 'A family of sensorless observers with speed estimate for rotor position estimation of im and pmsm drives'. Industrial Electronics Conf. (IECON 2012), Montreal, Canada, October 2012, pp. 3670–3675
23 Korlinchak, C., Comanescu, M.: 'Sensorless field orientation of an induction motor drive using a time-varying observer', *IET Electr. Power Appl.*, 2011, **6**, pp. 1–9
24 Proca, A.B., Keyhani, A.: 'Sliding-mode flux observer with online rotor parameter estimation for induction motors', *IEEE Trans. Ind. Electron.*, 2007, **54**, (2), pp. 716–723
25 Comanescu, M., Utkin, V.I.: 'A sliding mode adaptive MRAS speed estimator for induction motors'. IEEE Int. Symp. on Industrial Electronics, 2008, pp. 634–638
26 Lascu, C., Boldea, I., Blaabjerg, F.: 'A modified direct torque control for induction motor sensorless drive', *IEEE Trans. Ind. Appl.*, 2000, **36**, (1), pp. 120–130
27 Proca, A.B., Keyhani, A., Miller, J.M.: 'Sensorless sliding mode control of induction motors using operating conditions dependent models', *IEEE Trans. Energy Convers.*, 2003, **18**, (3), pp. 205–212
28 Chi, S., Zhang, Z., Xu, L.: 'A novel sliding mode observer with adaptive feedback gain for PMSM sensorless vector control'. Power Electronics Specialists Conf. (PESC), 2007, 17–21 June, pp. 2579–2585

doi: 10.1049/iet-epa.2013.0192